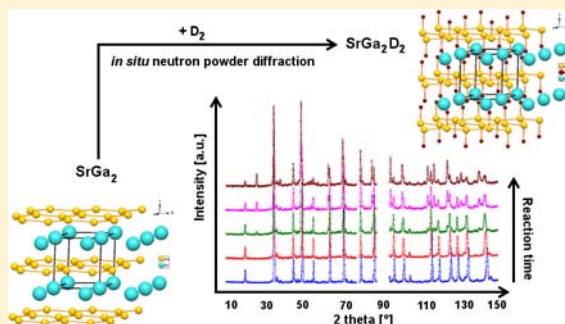


In Situ Neutron Powder Diffraction of the Formation of SrGa₂D₂, and Hydrogenation Behavior of YbGa₂ and EuGa₂Patrick Wenderoth[‡] and Holger Kohlmann^{*,†,‡}[†]Universität Leipzig, Institut für Anorganische Chemie, Johannisallee 29, 04103 Leipzig, Germany[‡]Universität des Saarlandes, Anorganische Festkörperchemie, Am Markt, Zeile 3, 66125 Saarbrücken, Germany

ABSTRACT: The hydrogenation behavior of the Zintl phases MGa₂ (M = Sr, Eu, Yb) was investigated. Upon being heated under 50 bar of hydrogen gas pressure, SrGa₂ starts forming the polyanionic hydride SrGa₂H₂ at 125 °C as observed by in situ differential scanning calorimetry (DSC) and ex situ X-ray powder diffraction. The deuteration of SrGa₂ was studied by in situ neutron powder diffraction at temperatures up to 300 °C in the pressure range of 50 ≤ p(D₂) ≤ 61 bar with a time resolution of two minutes. Neither incorporation of deuterium into the interstitials of the crystal structure of SrGa₂ nor any other intermediate of the reaction was observed. No significant variation in positional or occupational parameters as refined by the Rietveld method was observed for the deuteride SrGa₂D₂ under various temperature and pressure conditions (e.g., at T = 299 °C, p(D₂) = 60 bar, space group P $\bar{3}m1$, a = 4.4098(2) Å, c = 4.7429(3) Å, Sr in 1a, 0 0 0; Ga in 2d, 1/3 2/3 0.474(1); D in 2d, 1/3 2/3 0.120(2)). In situ DSC complemented by ex situ X-ray powder diffraction revealed that EuGa₂ and YbGa₂ do not form polyanionic hydrides in the investigated temperature–pressure ranges (20 °C ≤ T ≤ 220 °C, 5 bar ≤ p ≤ 54 bar). Instead binary hydrides and gallium-rich intermetallics are formed. The first refined crystal structural data are presented for YbGa₅ in the tetragonal PuGa₆-type structure (space group P4/nbm (No. 125), a = 6.0890(3) Å, c = 7.6562(4) Å, Yb in 2c, 3/4 1/4 0; Ga1 in 8m, 0.4750(4) 0.5250(4) 0.3377(4); Ga2 in 4g, 1/4 1/4 0.1691(5)).



1. INTRODUCTION

In this paper, results of in situ neutron powder diffraction (NPD) experiments on the Zintl phase SrGa₂ and its deuteride are presented. Also the related phases YbGa₂ and EuGa₂ were investigated with respect to a possible hydride formation.

All three compounds are Zintl phases structurally related to each other. SrGa₂ crystallizes in the hexagonal AlB₂-type, YbGa₂ in the hexagonal CaIn₂-type,^{1,2} and EuGa₂ in the orthorhombic KHg₂-type, which is very similar to the CeCu₂-type.^{1,3} In all of these structures, Ga forms graphite-like hexagonal layers, which are more or less distorted and connected or isolated. The Sr-, Yb-, or Eu-atoms are situated between the Ga layers (Figure 1). The structural relation can also be shown by the use of a Bärnighausen tree.⁴

Hydrides from Zintl phases can be categorized after Häussermann⁵ as either “Zintl phase hydrides” (e.g., CaSi–CaSiH_{1.0–1.3}) or “polyanionic hydrides” (e.g., SrAl₂–SrAl₂H₂). While the former contain hydride anions in interstitial positions, the latter are characterized by the presence of polyanions with homonuclear bonding to which the hydrogen atoms are covalently bound. Contrary to the hydrides with isolated [EH_n][−] units (e.g., borohydrides, alanes, and other), polyanionic hydrides are characterized by the presence of both E–E and E–H bonds.⁵

There are few other examples of polyanionic hydrides, such as MA₂SiH (M = Ca, Sr, Ba), SrGaGeH, BaGaTtH (Tt = Si, Ge, Sn),⁵ and RbGaH₂.⁶ In contrast to the Zintl phase hydrides, all of these known polyanionic hydrides seem to be stoichiometric with respect to hydrogen. Therefore, we would

Table 1. Experimental Conditions of in Situ DSC Experiments on the Hydrogenation of YbGa₂; Quantitative Phase Analysis by XRD of the Hydrogenated Products

hydrogen gas pressure [bar]	54	25	5
temperature ^a [°C]	220	180	180
	YbGa ₆ /29.7(5)%	YbGa ₂ /25.7(6)%	YbGa ₄ /6.0(7)%
phases/weight fraction	YbH _{2.67} /70.3(5)%	YbGa ₄ /57(1)%	YbGa ₅ /14.4(2)%
		YbGa ₆ /11(1)%	YbGa ₆ /45.9(5)%
		YbH _{2.67} /5.2(6)%	YbH _{2.67} /33.7(5)%

^aHeld each time for 2 h.

like to know whether any intermediate phases, for example, hydrides with lower hydrogen content than the fully hydrogenated product, form during the formation of these hydrides.

For SrGa₂, the existence of a corresponding polyanionic hydride SrGa₂H₂ is already known. It forms at about 50 bar of hydrogen pressure and 180 °C.⁷ Hydrides of the other compounds are not yet described in the literature, but because of the structural relationship, one can presume the existence of similar hydrides for EuGa₂ and YbGa₂.

2. EXPERIMENTAL SECTION

All samples were prepared from the metals. Gallium was obtained from ChemPur (pieces, 99.999%), ytterbium from Alfa Aesar (ingot, 99.9%),

Received: June 11, 2013

Published: September 4, 2013

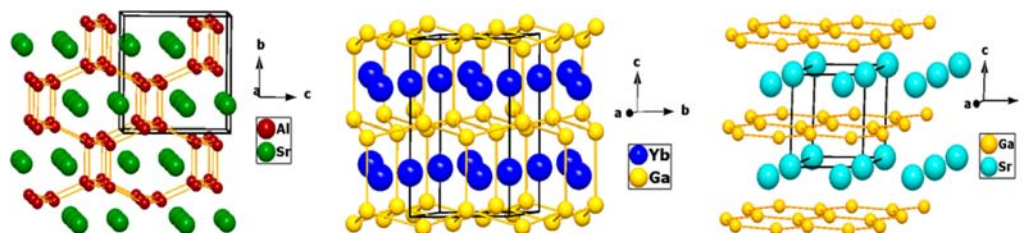


Figure 1. Structures of SrAl_2 (CeCu₂-type, left), YbGa_2 (CaIn₂-type, middle), and SrGa_2 (AlB₂-type, right).

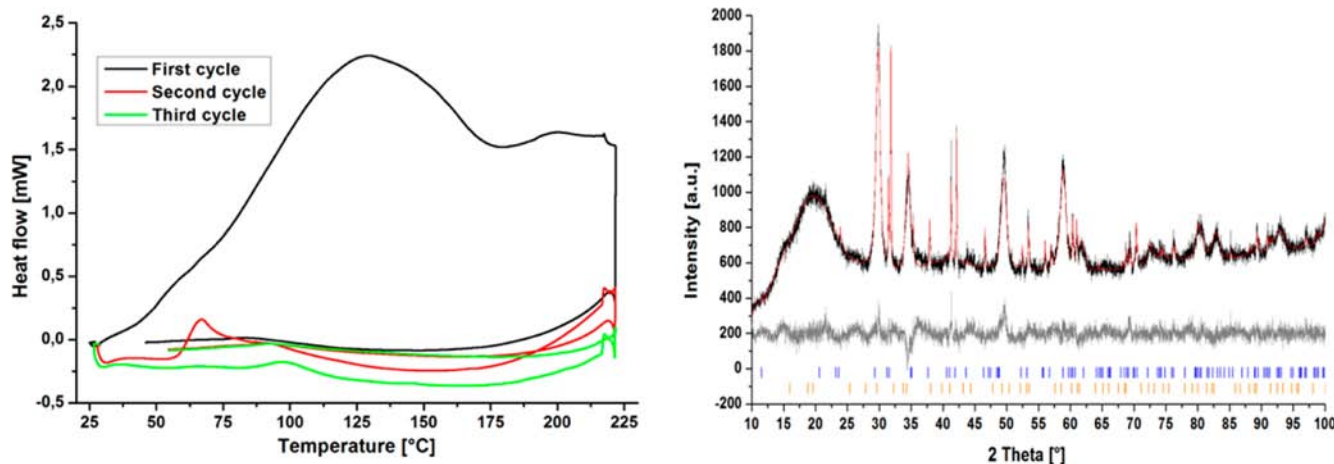


Figure 2. DSC diagram of YbGa_2 at 54 bar of hydrogen gas pressure and 220 °C for 2 h with exothermic signals in the positive direction (left) and X-ray powder pattern (Cu $K\alpha$) after the hydrogenation (right). Black is the measurement, red is the calculated curve, gray is the difference, and the Bragg markers from top to bottom are YbGa_6 and $\text{YbH}_{2.67}$.

Table 2. Refined YbGa_6 Crystallographic Data Prepared from DSC Experiments

		hydrogen pressure = 54 bar					hydrogen pressure = 5 bar				
space group		$P4/nbm$ (No. 125)									
a [Å]		6.0921(3)					6.0890(3)				
c [Å]		7.6590(4)					7.6562(4)				
V [Å ³]		284.25(3)					283.86(3)				
		hydrogen pressure = 54 bar					hydrogen pressure = 5 bar				
site	Wyck. letter	x	y	z	B_{eq}	x	y	z	B_{eq}		
Ga1	8m	0.477(1)	0.523(1)	0.3399(9)	1.0(2)	0.4750(4)	0.5250(4)	0.3377(4)	1.44(7)		
Ga2	4g	1/4	1/4	0.166(1)	1.0(2)	1/4	1/4	0.1691(5)	1.44(7)		
Yb	2c	3/4	1/4	0	1.0(2)	3/4	1/4	0	1.44(7)		
occupancy		all sites 100%					all sites 100%				
R Bragg		1.93					1.57				
R_{wp}		4.79					2.55				

europium from Gerresheim Lübeck (ingot, 99.98%), and strontium from Alfa Aesar (distilled dendritic pieces, 99.8% metals basis). All handlings were performed in an argon-filled glovebox. The oxide surface layers of the metals were mechanically removed, and the metals were cut to pieces for the reaction. Stoichiometric amounts of the elements were mixed in welded Nb ampules and either sealed in silica ampules or heated in a sublimation tube under vacuum. The samples were heated to 800 or 850 °C (Eu) for about 30 h. The Zintl phases were obtained as brittle products of gray color with a slight metallic luster, which were easily ground to gray powders.

Hydrogenation experiments were carried out in a TA Instruments Q1000 differential scanning calorimeter (DSC) equipped with a gas pressure cell at various hydrogen gas pressures in crimped aluminum pans with sample amounts of approximately 10–30 mg. To investigate the reversibility of the hydrogenation reactions, the DSC experiments were, for each sample, repeated once or twice without opening the cell. The heating rate for all the experiments was 5 °C/min. Additionally, for EuGa_2 and SrGa_2 , an autoclave machined from hydrogen-resistant Nicrofer 5219 Nb-alloy718 was used to prepare larger sample amounts. Hydrogen gas was obtained from Praxair (purity 99.9% or 99.999%).

Powder X-ray diffraction (XRD) data were taken with the use of a PANalytical XPert Pro diffractometer with PIXcel detector and Cu $K\alpha_{1/2}$ radiation in Bragg–Brentano geometry on flat samples enclosed between two kapton foils.

NPD experiments were carried out at the Institute Laue-Langevin in Grenoble, France, at high flux diffractometer D20 in high resolution mode with a time resolution of 2 min per pattern.

The sample was measured in a sapphire gas pressure cell⁸ and heated with the use of a laser heating system (2×40 W). The deuterium (isotopic purity 99.8%) pressure was controlled with the use of a gas pressure regulation system. The temperature was measured with the use of a pyrometer (Keller HCW PL 11 AF 3). A calibration for the temperature was made with palladium lattice parameters with respect to the temperature dependence found by Dutta and Dayal⁹ and given by eq 1.

$$T_{\text{cal}} = 8.0(7) \text{ °C} + 0.941(8) \cdot T_{\text{Pyro}} - 0.00029(2) \text{ °C}^{-1} \cdot T_{\text{Pyro}}^2 \quad (1)$$

For details of the experimental setup, see refs 8 and 10.

Table 3. Experimental Conditions of in Situ DSC Experiments on the Hydrogenation of EuGa₂; Quantitative Phase Analysis by XRD of the Hydrogenated Products

pressure [bar]	50	25	1
temperature ^a [°C]	180	180	180
phases/ weight fraction	EuGa ₂ /36.2(7)% Eu ₃ Ga ₉ /12.5(7)% EuGa ₄ /28.8(6)% Eu ₃ Ga ₈ /22(1)% EuO/–	EuGa ₂ /34.3(5)% Eu ₃ Ga ₉ /6.9(6)% EuGa ₄ /33.9(5)% Eu ₃ Ga ₈ /21.7(6)% EuO/3.3(4)%	EuGa ₂ /19.7(4)% Eu ₃ Ga ₉ /5.6(4)% EuGa ₄ /41.0(5)% Eu ₃ Ga ₈ /30.3(5)% EuO/3.5(4)%

^aHeld each time for 2 h.

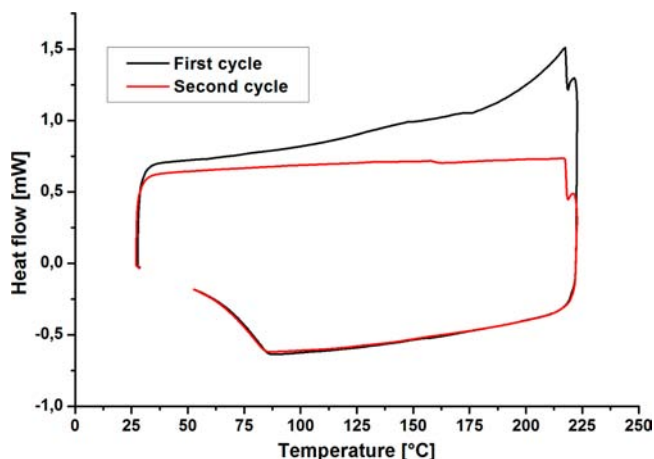


Figure 3. Heat flow curve of SrGa₂ at 50 bar H₂ pressure and 220 °C, held for 2 h, with exothermic signals in the positive direction.

The actual neutron wavelength, determined by a Rietveld refinement of a measurement of a NIST 640b silicon standard, was found to be 1.86765(5) Å. The Rietveld refinements of the XRD data were carried out with the programs TOPAS 2.1 and TOPAS 4.2,^{11,12} and for the refinement of the NPD data the program FULLPROF¹³ with pseudo-Voigt as the profile function was used.

3. RESULTS AND DISCUSSION

Hydrogenation Behavior of YbGa₂. The hydrogenation experiments were carried out with a single phase sample of

YbGa₂ and with a sample of YbGa₂ containing about 4 wt % of YbGa as a secondary phase.

The DSC measurements show exothermic reactions with different H₂ pressures. The conditions were 54 bar and 220 °C for 2 h; 25 bar and 180 °C for 2 h; and 5 bar, 180 °C for 2 h. As shown in Figure 2 (left), for the measurement with 54 bar, significant heat effects in the first and second repetition are not reversible upon cooling down. This is typical for the formation of metal hydrides in such in situ DSC experiments.¹⁴

In all the cases, the XRD diffraction data of the gray hydrogenation products were taken. Other than Ga-rich phases such as YbGa₄, YbGa₅, and YbGa₆, the data show only the formation of YbH_{2.67}. YbGa₅ seems only to form at low hydrogen pressure. For details about the identified phases see Table 1. Note that, in all cases, gallium is missing with respect to the nominal composition, so the weight fractions do not give the exact composition. Missing gallium can be assumed to be amorphous, to have concentrated in grain boundaries, or to have interacted with the aluminum pan used. In Figure 2 (right) a Rietveld plot for the product of the hydrogenation at 54 bar is shown.

Tagawa et al. and Pelleg et al. identified YbGa₆ crystals in the PuGa₆-type structure and reported the lattice parameters, but did not specify the atom coordinates.^{15,16} In our two DSC samples at 54 and 5 bar, the YbGa₆ peaks show only moderate overlap with that of the secondary phases. Thus, Rietveld refinements yielded structural parameters of reasonable accuracy even though there was no phase-pure sample available. There is no indication of incorporation of hydrogen into YbGa₆. We therefore consider the data given in Table 2 to describe the first refined crystal structure of YbGa₆.

Hydrogenation Behavior of EuGa₂. The hydrogenation of EuGa₂ was investigated with an autoclave experiment and with DSC experiments. The goal of the educt synthesis was only to produce a sample with EuGa₂ as a main phase, not to achieve pure single phase samples. Therefore, a sample consisting of 75.8(5) wt % EuGa₂ together with EuGa₄ (4.2(3) wt %), Eu₃Ga₉ (5.0(5) wt %), and Eu₃Ga₈ (15.0(3) wt %) was heated up to 300 °C under 90 bar of hydrogen gas pressure for 3 days in an autoclave. The resulting sample contained 85.1(8) wt % EuGa₄ and 14.9(8) wt % EuH₂ only.

The sample for the DSC experiments consisted of 63.6(5) wt % EuGa₂ together with Eu₃Ga₉ (5.6(4) wt %), EuGa₄ (17.2(3) wt %),

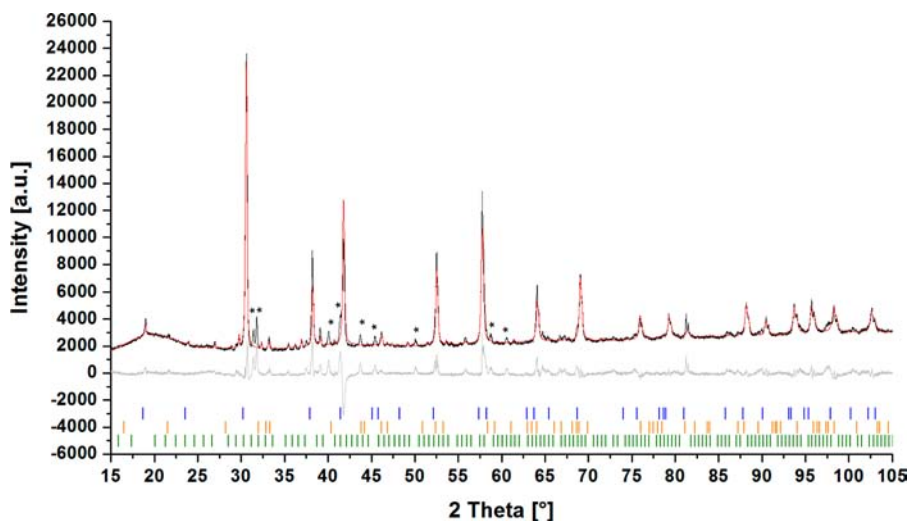


Figure 4. X-ray powder pattern (Cu K α), with Rietveld refinement, of SrGa₂ before the hydrogenation. Bragg markers are, from top to bottom, SrGa₂, SrGa₄, and Sr₈Ga₇. Some of the peaks assigned to the unidentified phase are marked with an asterisk.

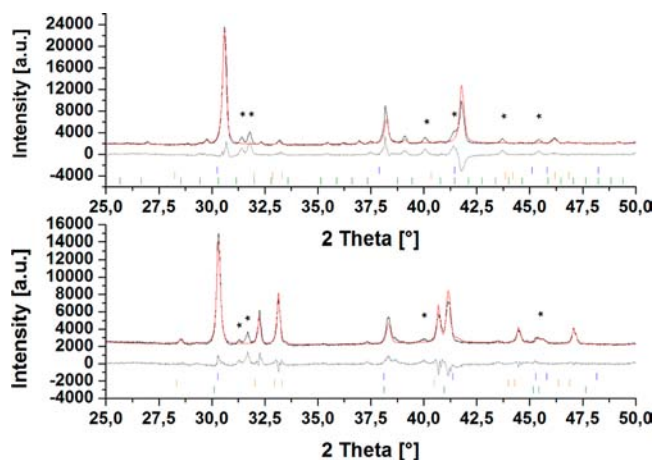


Figure 5. Detailed view of the X-ray powder pattern (Cu $K\alpha$) of SrGa_2 before (top panel) and after (bottom panel) hydrogenation in the DSC. Bragg markers are, from top to bottom, SrGa_2 , SrGa_4 , and Sr_8Ga_7 (top panel) and SrGa_2H_2 (bottom panel). Some of the peaks assigned to the unidentified phase are marked with an asterisk.

Eu_3Ga_8 (5.8(4) wt %) and EuO (7.9(2) wt %). Three conditions were chosen for the experiments: 50 bar of hydrogen gas pressure, 25 bar, and about 1 bar (i.e., purging only). Each experiment was heated to 180 °C and held for 2 h. Results of the experiments are given in Table 3.

Clearly, even without elevated hydrogen pressure, EuGa_2 decomposes into Ga-rich phases, so the weight fraction of these phases rises in all cases. Furthermore, EuO seems to be reduced by hydrogen at higher pressures. Thus, there is “missing” europium in all experiments; however, no further crystalline europium-containing phases are detected by XRD.

In conclusion, for EuGa_2 , results similar to those for YbGa_2 were obtained. EuGa_2 decomposes into EuGa_4 and EuH_2 . The Zintl phases EuGa_2 and YbGa_2 , in contrast to SrGa_2 , show oxidative decomposition, which has already been observed in other compounds, for example, in Ca_3Ga_5 , Li_3Al_2 , and SrZn_2 .¹⁷

Hydrogenation Behavior of SrGa_2 . The hydrogenation of SrGa_2 was examined with the use of high pressure DSC. Conditions were 50 bar of H_2 pressure and a maximum

temperature of 220 °C for 2 h. The heat flow curve is shown in Figure 3. The reaction starts at about 120 °C and has a strong increase of heat flow at about 180 °C. This is in agreement with the reaction conditions given by Björling et al. for the formation of SrGa_2H_2 .⁷ In the second cycle, no significant deviation from the baseline was detected, indicating that the hydrogenation reaction was already complete after the first cycle. The X-ray diffraction (Figure 4) of the SrGa_2 sample shows, before hydrogenation, weight fractions of SrGa_2 (90.3(4)%), SrGa_4 (1.5(2)%), and Sr_8Ga_7 (8.2(4)%), not including an unidentified phase.

After the hydrogenation, SrGa_2 was almost completely hydrogenated. The unidentified phase shows no reaction with hydrogen. Additionally, the weight fraction of SrGa_4 has increased, which may indicate the beginning of hydride decomposition. According to Björling et al.⁷ SrGa_2H_2 decomposes at higher temperature into SrGa_4 and SrH_2 . The binary hydride has perhaps not yet crystallized very well and therefore shows no peaks in the pattern. Weight fractions are 4.5(8)% for SrGa_2 , 36.9(4)% for SrGa_4 , and 58.6(6)% for SrGa_2H_2 . The Sr_8Ga_7 phase was not found anymore. A representative part of the XRD pattern before and after the sample was hydrogenated is shown in Figure 5.

In addition to the hydrogenation in the DSC, an experiment with the same parameters was done in an autoclave. The result was similar to that of the hydrogenation in the DSC, and a Rietveld refinement (Figure 6) led to the following weight fractions: SrGa_2 9.1(7), SrGa_4 34.2(5), and SrGa_2H_2 56.7(6).

In addition to the exploration and confirmation of the reaction conditions via DSC and autoclave, the hydride (deuteride) formation of SrGa_2 was investigated with in situ NPD. Deuterium gas was used to reduce the incoherent scattering of hydrogen. The reaction progress is shown in Figure 7. The sample was nearly phase pure, with little amounts of the aforementioned unidentified phase.

A comparison of the experimental with the calculated NPD patterns (Figure 7) shows that no intermediate product forms during the reaction, and the Zintl phase turns directly into the deuteride after half of the reaction time. At the end, SrGa_4 forms when the temperature reaches about 287 °C (small peaks rising at the end of the reaction time). In addition, the

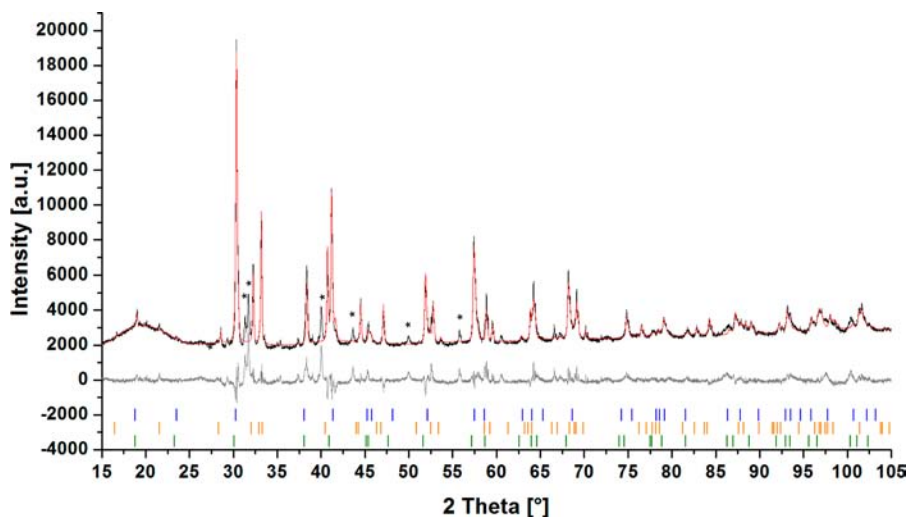


Figure 6. X-ray powder pattern (Cu $K\alpha$), with Rietveld refinement, of SrGa_2 after hydrogenation in the autoclave. Bragg markers are, from top to bottom, SrGa_2 , SrGa_4 , and SrGa_2H_2 . Some of the peaks assigned to the unidentified phase are marked with an asterisk.

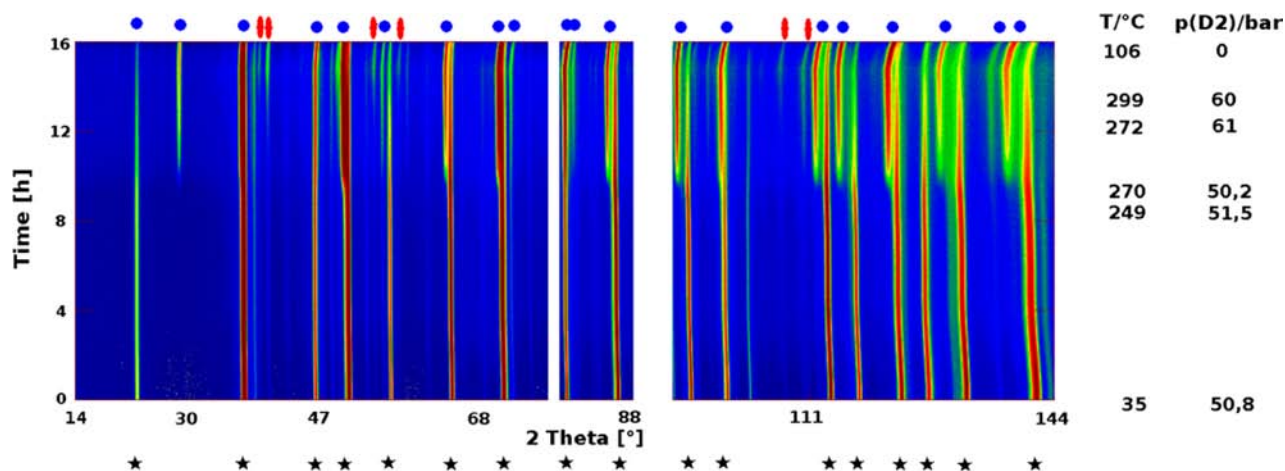


Figure 7. Time-dependent NPD patterns given in false colors (red = high intensity, blue = low intensity) showing the reaction progress of the deuteration of SrGa_2 . At about 78° and $90^\circ 2\theta$, peaks of the sapphire single crystal have been cut out. The refined wavelength is $1.86765(5) \text{ \AA}$. The patterns were recorded with a time resolution of 2 min/scan. The black asterisks below the picture mark the position of the SrGa_2 peaks; above the picture, the peak positions of SrGa_2D_2 are marked by blue circles, and the SrGa_4 peak positions are marked by red ovals. On the righthand side, temperature and the pressure of deuterium are given.

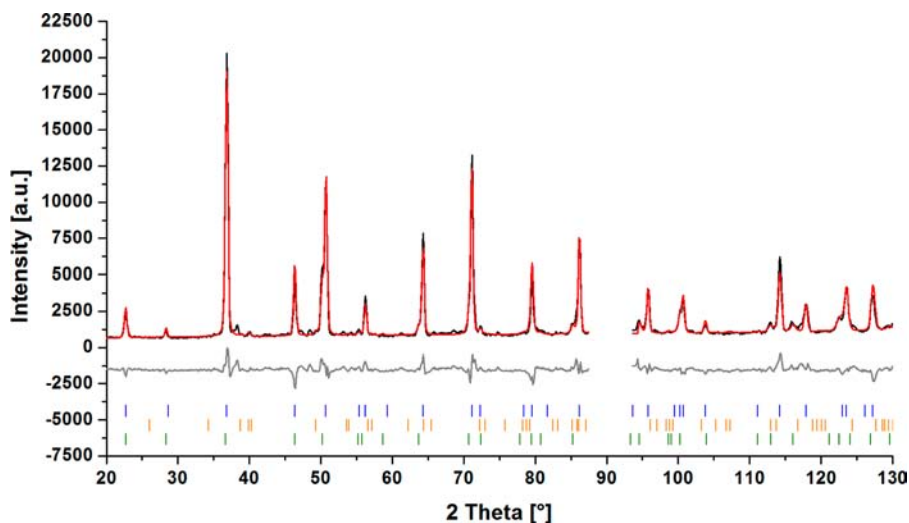


Figure 8. Neutron powder pattern ($\lambda = 1.86765(5) \text{ \AA}$) with Rietveld refinement at about 263°C . Bragg markers are, from top to bottom, SrGa_2 , SrGa_4 , and SrGa_2D_2 . The area cut out at about 90° in 2θ was excluded from the refinement and is the single crystal peak of the sapphire cell.

aforementioned unidentified phase continues to not react with hydrogen.

Figure 8 shows the Rietveld refinement at the start of the reaction, when the temperature is about 263°C . The deuteride formation is strongly indicated by the rising peak at about $30^\circ 2\theta$.

This is also confirmed by the nearly linear behavior of the lattice parameters, as shown in Figure 9. From the slope of the linear graphs in Figure 9, thermal expansion coefficients of $0.0029(1) \text{ \AA}^3 \cdot ^\circ\text{C}^{-1}$ for the Zintl phase SrGa_2 and $0.0050(1) \text{ \AA}^3 \cdot ^\circ\text{C}^{-1}$ for its deuteride can be determined, assuming, for each phase, a constant composition during the whole temperature range. These values represent typical thermal behavior for Zintl phases and hydrides (deuterides).¹⁸ Hydrogen (deuterium) incorporation on the other hand has a much larger effect on unit cell volumes, as can be seen by a comparison of the respective values for SrGa_2 and SrGa_2D_2 (Figure 9 and Table 4). Therefore, we conclude that no deuterium uptake takes place before the formation of the deuteride begins. After

cooling, the refined lattice parameters for the remaining SrGa_2 are not significantly different from those before the deuteration (a , $4.3483(2) \rightarrow 4.3504(3) \text{ \AA}$; c , $4.7404(2) \rightarrow 4.7372(6) \text{ \AA}$; both values at about 107°C), which further supports this conclusion. Because of uncertainties in the temperature, temperature gradients in the sample, and the general underestimation of estimated standard uncertainties (e.s.u.) by the Rietveld method, we consider the differences of 4.2 times the standard uncertainty for the lattice parameter a and 4.0 for that of c to be not significant.

In Table 4 the structural parameters of the SrGa_2D_2 phase at three selected times during the reaction are given as an overview. In contrast to the findings of Björling et al.,⁷ we found the deuterium occupation to be slightly below 1.0; however, the deviation from full occupation is only 3.3 e.s.u. In the same way, the positional parameters differ only slightly (maximum of 3.3 combined e.s.u. for $z(\text{D})$), which indicates that the crystal structure is rather rigid and not very susceptible to deuterium

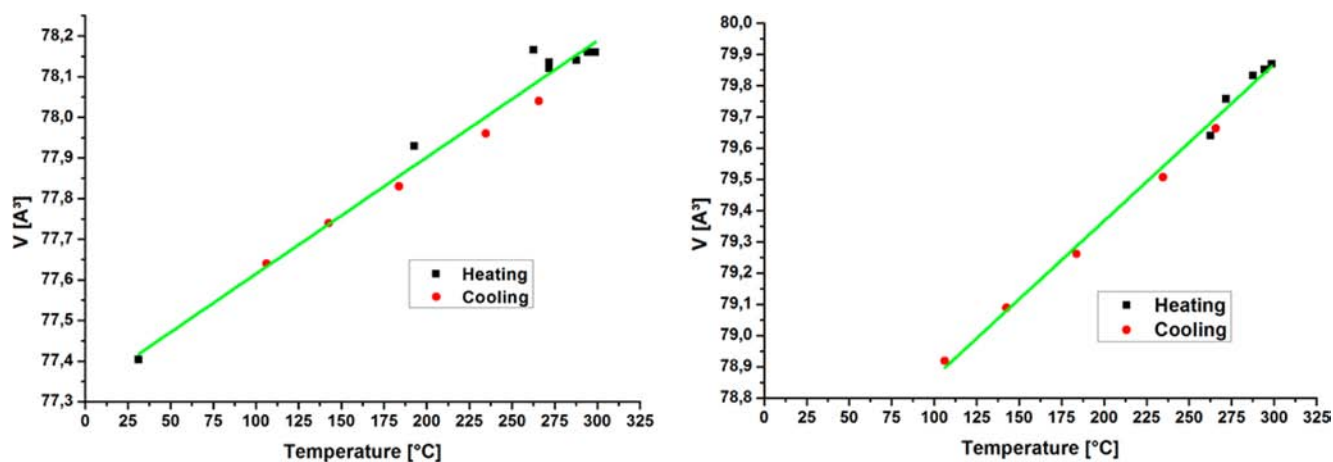


Figure 9. Refined unit cell volume of SrGa₂ (left) and SrGa₂D₂ (right) during the reaction progress. The data for heating (black) and cooling (red) are shown. Fitting each to a linear function yields $V = 77.33(3) \text{ \AA}^3 + 0.0029(1) \text{ \AA}^3 \cdot \text{°C}^{-1} \cdot T$ for SrGa₂ and $V = 78.36(3) \text{ \AA}^3 + 0.0050(1) \text{ \AA}^3 \cdot \text{°C}^{-1} \cdot T$ for SrGa₂D₂.

Table 4. Structural Parameters of the SrGa₂D₂ Phase at Selected Times from the Beginning of the Formation to the End of the Experiment

parameter	beginning of the reaction	end of heating	end of the experiment
T [°C]	272	299	106
p [bar]	54.5	60	1
space group	$P\bar{3}m1$ (No. 164)		
a [Å]	4.4077(2)	4.4098(2)	4.3969(2)
c [Å]	4.7409(4)	4.7429(3)	4.7138(2)
B (Sr), 1a: 0 0 0	2.8(4)	2.5(3)	1.8(2)
z (Ga), 2d: 1/3 2/3 z	0.477(2)	0.474(1)	0.472(1)
B (Ga)	1.2(2)	1.3(2)	0.7(2)
z (D), 2d: 1/3 2/3 z	0.125(2)	0.120(1)	0.115(1)
B (D)	2.1(3)	2.4(2)	1.6(2)
occupancy D-position	0.88(4)	0.90(3)	0.92(3)
d (Ga-D) [Å]	1.67(2)	1.680(9)	1.686(8)

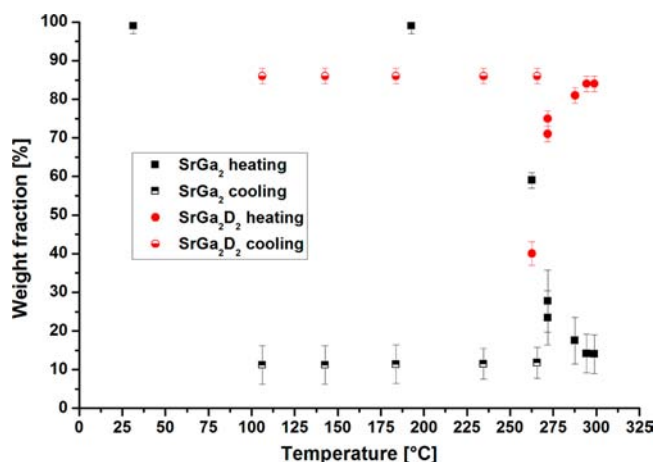


Figure 10. Weight fraction of SrGa₂ (black squares) and SrGa₂D₂ (red circles) during heating and cooling. The error bars represent 1 e.s.u.

gas pressure and temperature. Whether this hints of significant deuterium defects in the structure may be decided by independent experimental methods.

In Figure 10 the weight fractions of the gallide and the deuteride are shown; the fractions fall (and rise, respectively) rapidly after reaching a temperature of about 225 °C and

remain nearly constant after the reaction. Clearly, the hydrogenation process is incomplete. We assume that the sample amount is too big for the laser beam and so the sample is not completely heated. Additionally, the thermal conductivity of the sample may be low enough to cause a temperature profile together with the falling temperature effect of the laser beam.

4. CONCLUSION

SrGa₂ is known to form the polyanionic hydride SrGa₂H₂, in which hydrogen is bound covalently to the gallium polyanion.⁷ We have studied this hydrogenation reaction by in situ thermal analysis and in situ neutron diffraction. In the in situ DSC experiments at 50 bar hydrogen gas pressure, an exothermic peak with an onset around 125 °C indicates the formation of the polyanionic hydride. Temperature-dependent in situ NPD of the deuteration of SrGa₂ when heated to 300 °C in the pressure range of $50 \leq p(\text{D}_2) \leq 61$ bar shows a one-step reaction with no intermediate. SrGa₂ shows no sign of deuterium incorporation into its crystal structure before the reaction to SrGa₂D₂ takes place. The Rietveld refinement of the crystal structure of SrGa₂D₂ confirms the structural model reported earlier⁷ for each temperature–pressure condition studied. The refined deuterium-occupation parameters do not vary significantly and are close to unity; that is, a stoichiometric or nearly stoichiometric composition is assumed for SrGa₂D₂. In contrast to SrGa₂, the analogous and structurally related gallides EuGa₂ and YbGa₂ do not form polyanionic hydrides in the investigated temperature–pressure ranges ($20 \text{ °C} \leq T \leq 220 \text{ °C}$, $5 \text{ bar} \leq p(\text{H}_2) \leq 54 \text{ bar}$). Hydrogenation of YbGa₂ leads to the formation of binary ytterbium hydride, YbH_{2.67}, YbGa₄, YbGa₅, and YbGa₆, depending on hydrogen gas pressure and temperature. The first refined crystal structural data for YbGa₆ in the tetragonal PuGa₆-type structure are presented. Hydrogenation of EuGa₂ leads to the formation of binary europium hydride, EuH₂, and EuGa₄. These are further examples of the oxidative decomposition of Zintl phases upon hydrogenation, which competes with the formation of Zintl phase hydrides or polyanionic hydrides.

AUTHOR INFORMATION

Corresponding Author

*E-mail: holger.kohlmann@uni-leipzig.de.

Notes

The authors declare no competing financial interest.

■ ACKNOWLEDGMENTS

We thank the Deutsche Forschungsgemeinschaft (DFG) for funding of the project in the SPP1415, the Landesgraduiertenförderung Saarland (LGFG) for providing a scholarship, the Institut Laue-Langevin (ILL, Grenoble) for providing beam-time and Thomas Hansen for help with the instrument, Christian Reichert, Nadine Kurtzemann (Saarland University), Marc Widenmeyer (University Stuttgart) for experimental assistance, and Sylvia Beetz and Herrmann Recktenwald for technical assistance.

■ REFERENCES

- (1) Iandelli, A. *Z. Anorg. Allg. Chem.* **1964**, *330*, 221–232.
- (2) Palenzona, A.; Cirafici, S. *J. Phase Equilib.* **1992**, *13*, 32–35.
- (3) Sichevych, O.; Cardoso-Gil, R.; Grin, Y. *Z. Kristallogr.* **2006**, *221*, 261–262.
- (4) Hoffmann, R. D.; Pöttgen, R. *Z. Kristallogr.* **2001**, *216*, 127–145.
- (5) Häussermann, U. *Z. Kristallogr.* **2008**, *223*, 628–635.
- (6) Fahlquist, H.; Noréus, D.; Callear, S.; David, W. I. F.; Hauback, B. *C. J. Am. Chem. Soc.* **2011**, *133*, 14574–14577.
- (7) Björling, T.; Noréus, D.; Häussermann, U. *J. Am. Chem. Soc.* **2006**, *128*, 817–824.
- (8) Kohlmann, H.; Kurtzemann, N.; Wehrich, R.; Hansen, T. *Z. Anorg. Allg. Chem.* **2009**, *635*, 2399–2405.
- (9) Dutta, B. N.; Dayal, B. *Phys. Status Solidi B* **1963**, *3*, 2253–2259.
- (10) Widenmeyer, M.; Niewa, R.; Hansen, T. C.; Kohlmann, H. *Z. Anorg. Allg. Chem.* **2013**, *639*, 285–295.
- (11) *Topas, version 2.1, General profile and structure analysis software for powder diffraction data*, User Manual; Bruker AXS: Karlsruhe, Germany, 2003.
- (12) *Topas, version 4.2, General profile and structure analysis software for powder diffraction data*, User Manual; Bruker AXS: Karlsruhe, Germany, 2008.
- (13) Rodriguez-Carvajal, J. *FullProf 2.k*, version 5.20; ILL: Grenoble, France, 2011.
- (14) Kohlmann, H. *J. Solid State Chem.* **2010**, *183*, 367–372.
- (15) Tagawa, Y.; Sakurai, J.; Komura, Y.; Ishimasa, T. *J. Less-Common Met.* **1986**, *119*, 269–275.
- (16) Pelleg, J.; Kimmel, G.; Dayan, D. *J. Less-Common Met.* **1981**, *81*, 33–44.
- (17) Häussermann, U.; Kranak, V. F.; Puhakainen, K. Hydrogenous Zintl Phases: Interstitial Versus Polyanionic Hydrides. In *Zintl Phases: Principals and Recent Developments*, Fässler, T. F., Ed.; Structure and Bonding; Springer: Berlin, Germany, 2011; Vol. 990, pp 143–161.
- (18) Ting, V. P.; Henry, P. F.; Kohlmann, H.; Wilson, C. C.; Weller, M. T. *Phys. Chem. Chem. Phys.* **2010**, *12*, 2083–2088.